

Mirafs - Multi Image Resoulution Quality Acuminate Fusing System



John Livingston. S, Kumudha Raimond

Abstract: In Remote sensing applications, due to the increase in spatial and spectral resolutions, the time complexity became a vital aspect in order to process and deliver the solutions in a timely fashion. Remote sensors which acquire high-resolution image data often misses geometrical alignments and spectral stabilizations because of its dynamic routines, which results in crucial consideration such as loss of information and degraded quality in a single region of interest. This ignited us in finding the need for fusion of data to obtain quality products in remote sensing domain. Leaving the noise in source data compromises the overall quality of the solution. In proposed method to reduce the negative impacts of noise on the image skin, we use the confined filter function which held back the noise while reconstructing the image. In some cases, when image fusion is carried out using the least significant spectral band values will also lead to degraded output; in such condition, the Proposed method chooses high informative bands by careful attention to spectral values in each band. The anticipated outcomes through these methods are significant reduction in computational complexity and noise insensitivity. The fusion process must be verified to validate image sets for smart combinations of bands. The image pixels were considered as components to organize the fused spectral quality. The proposed HSI based MIRAFS method is compared with state of art fusion models and the results shows prominent improvement in the quality of fused images when we chose high spectral values. In MIRAFS, the quality of the resultant fused image has also been checked whether it has minimized spectral degradation with the amplified resolution by conserving spectral information as much as possible.

Index Terms: Fused Image; Noise; Spectral quality; Image Pixel.

I. INTRODUCTION

Sharp spectral images present enhanced information than blurred images. Though, in various conditions, it is not potential to gain completely clear focused spectral from remote places camera attempts, because some areas come out to be indistinct due to differences in the intensity of the shot and focus. This means if the image is focused by the camera at a single specific entity, a further region of the image can be out of coverage. A possible way of obtaining more images of the preferred scene of the similar position is with focal point centered on diverse essentials of the image. Then, by using the spectral fusion technique, all input images are combined,

generating a image that encloses all the greatest focused areas. Image fusion is suitable and especially popular with digital spectral dispensation. The varieties of tools are available and effectively working in the area of image dealing out. The main issues with graphical fusing technique are that the image sizes are huge, so the processing is deliberate. An image is fused as soon as we begin extracting output from it. An image generally goes from side to side some improvement steps, with the purpose of progressing the fusing data. A main flourishing technique of the principal component analysis (PCA) is(which)has been used in the image detection and firmness. The main aims of this multiple analysis were to decide the best pyramid technique deepness for the fusion of distantly observed image. This was resolute by investigating the identical set of inputs images fused upon a series of pyramid lowest point. In proposing, a complete image sketch can be observed by testing two input images constitution over a series of measure. When we expand an observed image, we obviously see the underneath; yet, we misplace the clearness of the image outlines. Conversely, when we expand out to appear at the complete image, the image misplaces feature. The initial aim of this analysis was to compare PCA image fusion methods, pyramid-based image techniques and to identify their efficiency in fusing satellite observation images based upon the merged image outputs. This was capable of relating the fusion methods of numerous experiment images and visually examining the image to detect fused image excellence. This was good by generating investigation images intended to illustrate specific outside skin and followed by fusing the input images to validate that the exterior features have been effectively fused. The paper is organized as follows: Section 2 deals with the Evolution of image fusion previous research, Section 3 describes the motivation of Image Fusion Techniques, Section 4 explains the MIRAFS image fusion method, Section 5 shows the result analysis, Section 6 explains the conclusion of the implementation.

A. Existing Reviews

These features from the source images are then fused to get the composite image. Decision level is a higher level of fusion where input images are processed individually for information extraction and the information was combined by applying decision rules to reinforce common interpretation [3]. The prime requirement was to develop truly effective processing techniques which could be implemented by geologists using inexpensive image processing systems [1]. The PCA technique in data dimension reduction is justified by the easy representation of multidimensional data, using the information contained in the data covariance matrix, principles of linear algebra and basic statistics [4].

Manuscript published on 30 August 2019.

*Correspondence Author(s)

John Livingston.S, Assistant Professor, Department of Computer Science and Engineering, Karunya Institute of Technology and Sciences, Coimbatore.

Kumudha Raimond., Professor, Department of Computer Science and Engineering, Karunya Institute of Technology and Sciences. Coimbatore.

© The Authors. Published by Blue Eyes Intelligence Engineering and Sciences Publication (BEIESP). This is an [open access](http://creativecommons.org/licenses/by-nc-nd/4.0/) article under the CC-BY-NC-ND license <http://creativecommons.org/licenses/by-nc-nd/4.0/>

The simplest methods in the spatial domain used a weighted arithmetic mean of the source image pixels intensity this method is associated with an image blurring and decreasing the image contrast. Multi-scale image fusion methods are very common and convenient [9]. The transformation representation is particularly unsuited for machine vision and computer graphics, where the spatial location of pattern elements is critical[6]. Aspect that distinguishes the layer separation problem from image decomposition approach is the fact that one of the layers may obstruct another layer in large parts of an image, thus blocking features in an obstructed layer [2]. These methods automatically combine an occasionally large step that may severely violate the forward Euler absolute stability restriction but yields rapid convergence with small steps that restore stability and smoothness [7]. Image fusion in pixel level refers to generating of fused image in which the pixel values are based on the pixel values of the source image. Feature-based fusion requires the extraction or segmentation of various features of the source images [5]. The main task of the algorithm is to determine a pixel belonging to an object by comparing it with the average intensity of the pixels classified as an area, wherein the size of the acceptance interval is dependent on the intensity factor taking into account the variability of the environment [8].

B. Motivation

Image Fusing Techniques Of PCA

The PCA imaged fusion read the principle components from the input images and merges the image factors of eigen-spaces. The pixel values of the input image are retrieved using the image read function and the values are converted into 3-dimension matrices as RGB color spaced values.

$$I1 = \begin{pmatrix} R \\ G \\ B \end{pmatrix} \begin{pmatrix} r_{11} \dots r_{12} \dots r_{13} \\ r_{21} \dots r_{22} \dots r_{23} \\ r_{31} \dots r_{32} \dots r_{33} \end{pmatrix} \begin{pmatrix} g_{11} \dots g_{12} \dots g_{13} \\ g_{21} \dots g_{22} \dots g_{23} \\ g_{31} \dots g_{32} \dots g_{33} \end{pmatrix} \begin{pmatrix} b_{11} \dots b_{12} \dots b_{13} \\ b_{21} \dots b_{22} \dots b_{23} \\ b_{31} \dots b_{32} \dots b_{33} \end{pmatrix} \quad (1)$$

$$I2 = \begin{pmatrix} R \\ G \\ B \end{pmatrix} \begin{pmatrix} r_{11} \dots r_{12} \dots r_{13} \\ r_{21} \dots r_{22} \dots r_{23} \\ r_{31} \dots r_{32} \dots r_{33} \end{pmatrix} \begin{pmatrix} g_{11} \dots g_{12} \dots g_{13} \\ g_{21} \dots g_{22} \dots g_{23} \\ g_{31} \dots g_{32} \dots g_{33} \end{pmatrix} \begin{pmatrix} b_{11} \dots b_{12} \dots b_{13} \\ b_{21} \dots b_{22} \dots b_{23} \\ b_{31} \dots b_{32} \dots b_{33} \end{pmatrix} \quad (2)$$

$$I1 \Sigma = (R \ G \ B), \quad I2 \Sigma = (R \ G \ B) \quad (3)$$

$$\Sigma I1 = (\sum R \dots \sum G \dots \sum B), \quad \Sigma I2 = (\sum R \dots \sum G \dots \sum B) \quad (4)$$

In Eq (1) to (7) Where R,G,B denoted as red, green, and blue colors. Estimate the mean (M) value for 2 input images.

$$MI1 = \frac{\Sigma}{(R,C)}, \quad MI2 = \frac{\Sigma}{(R,C)} \quad (5)$$

Convert PCA Component to RGB

$$I1 = (R \dots G \dots B) \quad I2 = (R \dots G \dots B) \quad (6)$$

$$BV = (R \dots G \dots B) \begin{pmatrix} R \\ G \\ B \end{pmatrix} \quad (7)$$

For each pixel value of the RGB scale, the sum of the pixel values is computed for the transformed matrix (TF) and the

value is estimated at both input images. From the sum value and size of the matrix, an average pixel value is computed as a first principle component. The second principle component is computed as covariance (C) which requires two inputs as represented in Eq (8).

$$C = ([R \ G \ B]) / ((R \times C)) \quad (8)$$

The first input is computed as average pixel values of the product matrix with the transformed vector matrix and it is computed from the pixel values of both the images as the sum of a product of input vector matrix with the transformed vector matrix then the value is divided by the number of pixel points present in the image. The second inputs are computed as a product of the average pixel value and the inverted average pixel value. Eq (9) gives the difference between the two inputs is computed as C matrix and given as input to the eigen-function (EF).

$$EF = ((I1 \cdot C) - (I2 \cdot C)) \quad (9)$$

The eigen-function provides the eigen-value of both input image vector by applying the eigen-equation solving method as. From Eq. (10), the two eigen-value of the image vectors, average values are computed in three color spaces in the transformed matrix. Average of the eigen-value and the average value of the three-color space are multiplied by the color vectors of the fused image (FI).

$$((R+R)/2) \ ((G+G)/2) \ ((B+B)/2) = ((EF1 + EF2)/2) \quad (10)$$

Update final fused image (FFI) = . This produces PCA fused image The 3D color space of the fused vectors is combined to form the fused image shown as output in Figure 1C.

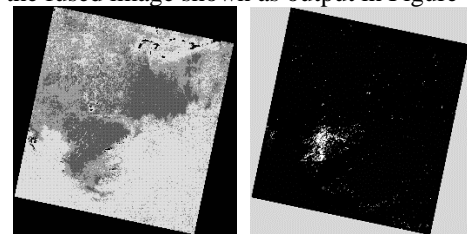


Figure 1A, 1B. Input Images

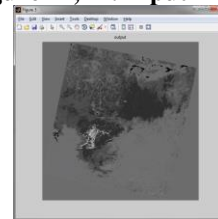


Figure 1C. Input Image Fusing Techniques Of PYRAMID

The Laplacian pyramid is used to merge the feature of the two images to produce the fused image of the multi-level components. The inputs images are read, and the pixel values are stored in two different arrays of processing as with RGB components. The pixel values are divided into the RGB scale of 3-dimension matrices as 3 color scales of the image.

In order to form the pyramid structure, the principal components are extracted from the RGB color vector with the 2-dimension concatenation operator applied to the input image. Eq. (11) represents the weight value of the vectors (V) is computed by using the normalization function by dividing the values by its sum of values. Where. IPV and TV are independent vectors and total vector respectively.

$$V=IPV/TV \tag{11}$$

The transformed vector is computed by multiplying the weight value of extracted principle component vector. The transformed vector is in the form of 3d dimension for three color spaces and these values are combined as a final transformed vector. The final transformed vector is computed for both input images, and from the vector, the chrominance component is computed by taking the average value of the chrominance component in both images. To compute the Luminance component, the image vector is reduced in 2D and expanded upon 3D. This will result from the round of value of the vector.

$$ID1 = (Image1 - 2D) \tag{12}$$

$$ID2 = (Image2 - 2D) \tag{13}$$

$$D = ID1 - ID2 \tag{14}$$

Eq. (12) to (13) gives the difference (D) between the original vector and the round of vector is computed as normalization factor when compared with both imaged vectors. The maximum weight value of the normalization factors is selected from both images and it is used to estimate the inverted document frequency of the combined image.

$$Weight = |ID1 - ID2| \tag{15}$$

The average value of the Luminance vector in both the images are computed for the fused image and the estimated inverted document frequency (IDF) is merged with the luminance vector of the fused image.

$$IDF = (D \times ID1) + (D \times ID2) \tag{16}$$

After identifying the Luminance and chrominance factor of both images, the principle component to the RGB component conversion is performed with the vectors of the original image as reference vectors. The computed RGB components of the two images are merged to create the final fused image. $V \rightarrow RGB$

Proposed MIRAFS Implementation Techniques

Hyperspectral imaging classifications are broadly used in ground monitoring systems and provincial applications. A HSI based MIRAFS spectral computation provides complete image information that allows the viewer to notice and categorize a pixel based on its image observation. The hyperspectral image fusion is implemented based on the bandpass filter (BPF) operation which requires the merging process of the low pass (LPF) and high pass filters (HPF). HPF and LPFs are used in image processing to carried out image adjustments, developments, noise cutback, and so on, using plans done in either the spatial field or the frequency field. The sharp-less or clear, process used in image suppression is a high increasing filter, a simplification of HPF. They satisfy all frequencies lower than an occurrence and upper than an occurrence, while the frequencies connecting the two cutoffs stay in the resultant output. The pixel values of the input image are stored in 3D array and it is given as input to the filter operation. In the

frequency domain, the high pass filter operation is applied to the pixel arrays by calculating the unit difference between negative exponent values of the ratio of the powered current pixel value of the cutoff frequency. Eq. (17) to (22) helps in computing the BPF value. The cutoff frequency (CF) is computed as an average value of the pixel matrix.

$$CF = Image1(i, j) \tag{17}$$

$$LPF = 1 - \frac{(CF)^2}{(CF \times 2)} \tag{18}$$

$$HLP = (1 - LPF) \tag{19}$$

The operator for the low pass filter is computed as the inverted difference between the high pass filter operations.

$$D = Image2(i, j) \tag{20}$$

$$HHP = (1 - HPF) \tag{21}$$

The band pass filter operation is applied by taking the product of LPF value and HPF value.

$$BPF = LPF \times HPF \tag{22}$$

The intensity of the image is computed for the band pass filtered output by computing the average of a sum of RGB scale values. The intensity computation is performed for both input images and the color component Hue is estimated as angle variable by taking the arctan function of the ratio intensity(I) values.

$$II1 = \frac{(RS+GS+BS)}{3}$$

$$II2 = \frac{(RS+GS+BS)}{3} \tag{23}$$

The calculations have been respectively represented from Eq.(23) to (29). The combined intensity is estimated as the average of intensity values.

$$\tan \phi = \frac{II1}{II2} \tag{24}$$

$$\phi = \text{atan} \frac{I1}{I2} \tag{25}$$

$$I = 0.5 \times (I1 + I2) \tag{26}$$

$$X1 = I \cos(\phi) \text{ single image} \tag{27}$$

$$X2 = I \sin(\phi) \cos(\phi) \text{ Two image}$$

$$\text{Final } X = I \times \sin(\phi) \times \cos(\phi)$$

$$Image = RGB \rightarrow HSV \tag{28}$$

Where X is colors pace hue. Now the input image is processed in 3D as hue saturation and value then the Haar transform is applied to regulate the image signal along with the 2dimension discrete wavelet transform. Converted to wavelet(W) transformation as related Values as (h, v, d)

$$II1 = [a, \dots, h1, v1, d1]$$

$$II2 = [a, \dots, h2, v2, d2]$$

$$A1 = \sum \frac{h1}{a} \quad A2 = \sum \frac{h2}{a} \tag{29}$$

$(A1 > A2) Temp = (h1, v1, d1) else (h2, v2, d2)$

In the HSV scale, the wavelet function provides the coefficient value and the Color-space values as shown in Figure 2

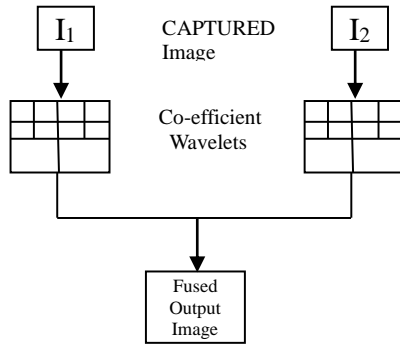


Figure 2. Image Fusing Structure

Each color space value is divided by the coefficient to compute the normalized vector in the current color space. And the sum of the normalized vector is computed for both input images and compared to the exact color space value which provides the color space value of the fused image of the color vector.

$$Intensity = \frac{I1+I2}{2} \tag{29}$$

Eq. (30) gives the average of the coefficient (C) is computed for the filtered image as the coefficient of the fused image.

$$C = \frac{C1+C2}{2} \tag{30}$$

The same operation is repeated for HSV a color space which provides the output in the form of haar transformed wavelet with the coefficient and color space values. The estimated coefficient and the color space values are combined using the 2dimension inverse discrete wavelet transform which results from the fused image.

$$(W = (Temp) \rightarrow w \rightarrow (RGB)$$

The fused image is validated for the unwanted noise portion and the noise pixel value is removed by copying the value of horizontal, vertical or a diagonal pixel value.

$RGB \rightarrow ImageOutput$ as like Figure 3

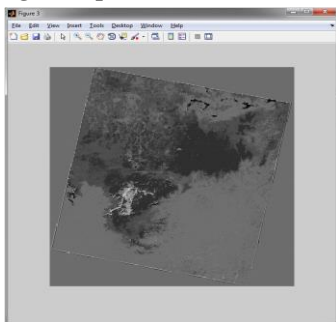


Figure 3 MIRAfS Fused Image Output

Result Analysis

Here we have used the snapshots of land images taken from the sight of a spectral database. The image database of the different land images presents in the photo shot region like earth and land. Two types of fused techniques have been tested and compared with the MIRAfS because of its image resolution.

In computation, the mean squared error difference between an assessment of a method of calculating an

unnoticed size measures the mean of the squares of the fault and variations that is, the dissimilarity between the calculation and what is calculated. In this illustrated graph shown in Figure 4, minimum error deviation had shown in proposed MIRAfS than the existing PCA and Laplacian methods.

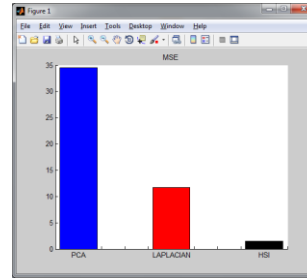


Figure 4 MSE

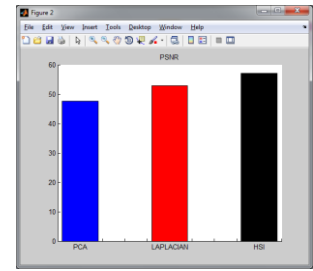


Figure 5 PSNR

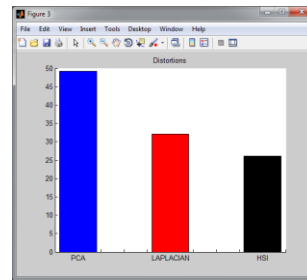


Figure 6. Distortion

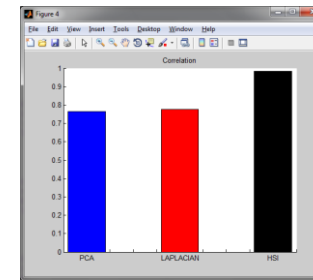


Figure 7 Correlation

The peak signal to noise ratio chunk estimated in decibels, involving input images. This relation is frequently used as an excellence dimension between the images with superior in the PSNR, the improved worth of the rebuild image. In output Figure 5 shows the improved PSNR in MIRAfS. In arithmetic computations, distortion is a difference from rectilinear outcrop depends on focal point, this brings bend of images – evenly and clearly; an outcrop in which direct lines in a sight stay without delay in an image. Outlook distortion is origin by the point of the sensor direction to the image or by the angle of the image inside the frame and need to classify the distortion. In Figure 6. MIRAfS shows the minimum distortion than the existing computations. In correlation, the assessment of a pixel is also computed as a subjective sum of nearby pixels. The dissimilarity is that the matrix of subjects in this case calls the *connection core*, is not rotated throughout the calculation. In this Figure 7 MIRAfS shows the higher correlation points than the previous methods.

II. CONCLUSION

As we have discussed in result analysis the proposed method offers a prominent result in increasing the fusion performance over the state of art algorithms by carefully choosing high spectral quality band values. When the input data contains high spectral information then the quality of fused image increases. There has been a marginal difference in performance when there is spectral degradation in the input image. Result also shows that this can be improved through inbound features identified in given input image band values.



Further research is also possible when alternative transform methods combined with performance tuning used in satellite data will enhance the quality of the product in the spatial and spectral domain.

ACKNOWLEDGMENT

We acknowledge the USGS.gov(United states geological survey) for providing access to National Land Cover Database (NLCD) in accessing source data.

REFERENCES

1. W. P. Loughlin, "Principal Component Analysis for Alteration Mapping" Photogrammetric Engineering Remotesensing, vol. 57, no. 9, september 1991. pp. 1-3
2. Igor Yanovsky, Anthony B. Davis, Veljko M. Jovanovic, "Multilayer Separation and its Application to Separating Layers of Clouds" UCLA CAM Report, 2011. pp. 113-121
3. Amina Saleem, Azeddine Beghdadi and Boualem Boashash, "Image Quality Metrics Based Multi-focus Image Fusion" IEEEM, 2011. pp. 131-137
4. Rafael do Espirito Santo, "Principal Component Analysis applied to digital image compression" ORIGINAL ARTICLE, published was due on Jun 13, 2012.
5. A. Anish, T. Jemima Jebaseeli, "A Survey on Multi-Focus Image Fusion Methods" International Journal of Advanced Research in Computer Engineering & Technology (IJARCET) Volume 1, Issue 8, October 2012.
6. Binod kumar Choudhary, Navin kumar Sinha and Prem shanker, "Pyramid Method in Image Processing" Journal of Information Systems and Communication, Volume 3, Issue 1, 2012.
7. Hui Huang, Uri Ascher, "Faster gradient descent and the efficient recovery of images" 12 Aug 2013.
8. Ewelina PIEKAR, Michal MOMOT, Alina MOMOT, "Segmentation of Images Using Gradient Methods and Polynomial Approximation" JOURNAL OF MEDICAL INFORMATICS & TECHNOLOGIES Vol. 23, 2014.
Mostafa Amin-Naji, Ali Aghagolzadeh, "Multi-focus image fusion using VOL and EOL in DCT domain" International Conference on New Research Achievements in Electrical and Computer Engineering (ICNRAECE), May 13, 2016.
9. R. J. Vidmar. (1992, August). On the use of atmospheric plasmas as electromagnetic reflectors. *IEEE Trans. Plasma Sci.* [Online]. 21(3). pp. 876-880. Available: <http://www.halcyon.com/pub/journals/21ps03-vidmar>
10. Alphy George, John Livingston.S "A Survey on Full Reference Image Quality Assessment Algorithms" International Journal of Research in Engineering and Technology Vol.2, Issue.12, pp. 303-307, Dec. 2013
11. S. Arokia Jerome George, John Livingston.S "Survey on Region Growing Segmentation and Classification for Hyperspectral Images" International Journal of Computer Applications (0975 - 8887) Volume 62- No.13 January 2013

AUTHORS PROFILE



Mr. John Livingston.S, M.Tech.,(Ph.D) is working as a Teaching faculty in department of Computer science and Engineering Karunya University, Coimbatore, South India. His area of research is Big data analytics, Image analysis and Interpretation. He is also an Associate member of IEI



Prof/Dr. J. Kumudha Raimond is currently working as Professor, Department of Computer Sciences and Engineering, Karunya Institute of Technology and Sciences. India. Her research has included Bioinformatics, Biomedical Applications, Image Processing, Watermarking, MANET Protocols, Wireless Sensor Networks. She is an esteemed member of IEI